C.P. No. 643

LIBRARY
ROYAL AIRCRAFT ESTABLISHMENT
BEDFORD.

C.P. No. 643

MINISTRY OF AVIATION

AERONAUTICAL RESEARCH COUNCIL

CURRENT PAPERS

Low Speed Wind Tunnel Tests on a Kite Balloon Model

by

M. H. Simonds, B.Eng.

LONDON: HER MAJESTY'S STATIONERY OFFICE

1963

PRICE 2s 6d NET

U.D.C. No. 533.63 : 533.6.013.1 : 533.6.013.4

C.P. No. 643
November, 1961

LOW SPEED WIND TUNNEL TESTS ON A KITE BALLOON MODEL

by

M. H. Simonds, B.Eng.

SUMMARY

Low speed wind tunnel tests, aimed mainly at finding certain lateral aerodynamic stability derivatives, were carried out on a rigid 1/80th scale model of a 70600 cu ft kite balloon. The lift, drag and pitching moment, and the variation with angle of sideslip of the static values of side force and yawing moment, were found. In dynamic tests, the aerodynamic damping of free oscillations in yaw was measured about three separate axes of rotation. From these measurements the following combinations of stability derivatives were found: $(n_r - n_{\dot{v}})$, $(n_v - y_{\dot{v}} + y_r)$ and y_v. Results were obtained for the model at zero incidence, with the fins in place and with them removed.

Replaces R.A.E. Tech. Note No. Aero.2799 - A.R.C. 23,692.

LIST OF CONTENTS

		Page
1	INTRODUCTION	3
2	DESCRIPTION OF TESTS	3
3	DISCUSSION OF RESULTS	4
LIST OF SYMBOLS		5
LIST OF REFERENCES		7
APPENDIX -	Expression for the aerodynamic yawing moment when the model is rotated about different axes	8
ILLUSTRATIONS - Figs.1-7		-
DETACHABLE ABSTRACT CARDS		-

LIST OF ILLUSTRATIONS

	Fig.
The dynamic test rig	1
Positions of the axes of rotation	2
Reference axes and rotation	3
Lift, drag and pitching moment	4
Variation of yawing moment with sideslip	5
Variation of side force with sideslip	6
Aerodynamic damping in yaw about various axes of rotation	7

1 INTRODUCTION

The use of kite balloons as steady platforms in the sky has hitherto not been possible, since existing types suffer from large scale wander. For example, the 19150 cu ft balloon of Ref.1 on a cable length of 920 ft, had a lateral wander over a distance of 500 ft, and lateral velocities of 70% of the wind speed were measured.

Regardless of whether balloons could ever be developed which could fly effectively motionlessly with respect to the ground in an atmosphere which is never at rest, it was felt that there was room for improvement in balloon design to achieve more stable flight. For lateral dynamic stability analysis of kite balloons[2], values of lateral aerodynamic stability derivatives were required, and the main purpose of the low speed tunnel tests was to obtain these and to assess the respective contributions of the body and fins to them.

2 DESCRIPTION OF THE TESTS

The model was a 1/80th scale model of a 70600 cu ft kite balloon. It was constructed of pine and had balsa fins, and was therefore effectively rigid. The surface was roughened all over with carborundum dust to ensure early and complete transition. The model was made so that it could be fitted to the dynamic test rig at three separate positions. Leading dimensions and the positions of the axes of rotation are shown in Fig.2.

A diagram of the dynamic test rig appears in Fig.1. The model is mounted on the end of a shaft, which is supported on cross spring pivots and has its axis normal to the stream. The shaft projects through the tunnel wall, and outside the tunnel a transverse rocking beam is rigidly attached to it; this beam is elastically constrained by coil springs attached by fine wires to its ends. The aims in designing this rig were that the motion of the model should accurately be rotational yawing about a fixed axis, that the elastic constraint to this rotation should not vary with load, and that the rig damping should be small and repeatable.

Strain gauge balance measurements of rather poor accuracy were made of the forces and moments on the complete balloon model. Of these, the lift, drag and pitching moment at zero sideslip are shown in Fig.4. The dynamic test rig was used statically to measure the variation of yawing moment with sideslip about the two extreme axis positions (axes 1 and 3) at zero incidence. This was done for both the complete balloon model and the model with fins removed, and the results are shown in Fig.5. The variation of side force with sideslip was inferred from these results, and plotted in Fig.6.

The dynamic tests consisted of measuring the rate of decay of free oscillations. There was a capacitor type transducer for measuring the angular displacement, and records of the decaying oscillations were made on paper using a galvanometer recorder. The aerodynamic damping in yaw was found about the three separate axes.

With reference to Fig.3, if the model is oscillating in yaw about a fixed axis A a distance x_A aft of the origin O, to which the motion, forces, moments and stability derivatives are referred, then the equation of motion of the free oscillations is:-

$$(I - N_{\dot{\psi}}) \ddot{\psi} + (\sigma - N_{\dot{\psi}}) \dot{\psi} + (K - N_{\psi}) \psi = 0 \qquad (1)$$

where I = moment of inertia of model and moving parts of rig about A

σ = rotary damping factor of the rig

K = rotary stiffness of the rig

The expressions for the aerodynamic moment derivatives appearing in (1), as derived in the appendix, are:-

$$N_{\dot{\psi}} = N_{\dot{r}} + x_A Y_{\dot{r}} + x_A (N_{\dot{v}} + x_A Y_{\dot{v}}) \qquad (2)$$

$$N_{\dot{\psi}} = N_r + x_A Y_r + x_A (N_v + x_A Y_v) - U(N_{\dot{v}} + x_A Y_{\dot{v}}) \qquad (3)$$

$$N_{\psi} = - U(N_v + x_A Y_v) \quad . \qquad (4)$$

For this rig, $N_{\dot{\psi}}$ and N_{ψ} are very small compared with I and K, respectively. This means that the change in frequency of the free oscillations between wind-off and wind-on conditions is too small for anything useful to be deduced from it. In any case, there is a fundamental indeterminacy in such frequency measurements, since the change depends on both N_{ψ}/K and $N_{\dot{\psi}}/I$. In this experiment, it is only the aerodynamic damping which has been found.

The dimensional formula for the aerodynamic damping derivative $N_{\dot{\psi}}$ can be rewritten:

$$N_{\dot{\psi}} = N_r - U N_{\dot{v}} + x_A(N_v + Y_r - U Y_{\dot{v}}) + x_A^2 Y_v \quad . \qquad (5)$$

Non-dimensionalising, by dividing through by $\rho U S \ell^2$, we obtain

$$n_{\dot{\psi}} = n_r - n_{\dot{v}} + \frac{x_A}{\ell} (n_v + y_r - y_{\dot{v}}) + \left(\frac{x_A}{\ell}\right)^2 y_v \quad . \qquad (6)$$

Thus in principle, for lateral motion which is adequately described by these linear equations, a knowledge of the aerodynamic damping about three separate axes means that a "damping parabola" may be plotted, the coefficients of which are the following groups of stability derivatives $(n_r - n_{\dot{v}})$, $(n_v + y_r - y_{\dot{v}})$ and y_v. Damping parabolas for the model with and without fins have been plotted in Fig.7.

3 DISCUSSION OF RESULTS

In considering the results of these tests, insofar as they apply to full scale kite balloons, the following limitations should be borne

in mind. The model was rigid, and the scale and hence Reynolds number was very small. However, for the dynamic tests, the frequency parameters were chosen to be of the same order as those of the observed motions of full sized kite balloons. No correction has been made for tunnel blockage or the interference of the shaft and its fairing.

From Fig.6, it can be seen that the presence of the fins is responsible for the major part of the side force on the complete model. The centre of pressure of the static side forces on the complete model is 0.44 ℓ aft of the nose, whilst for the body of revolution with fins removed, the centre of pressure is 0.08 ℓ ahead of the nose.

The important results of the dynamic tests are summarised in the graph of Fig.7. The graph shows two damping parabolas, one for the complete model, and the other for the model without fins. The aerodynamic damping of the model without fins was only a small proportion of the damping of the complete model. Tests were carried out at zero incidence for two not very different frequency parameters (the same physical frequency of about 3 c.p.s. and two wind speeds U = 60 ft/sec and U = 100 ft/sec): the variation of the dampings between these two frequency parameters was barely distinguishable from the experimental scatter, so that the damping parabolas were plotted using average values of the damping.

An interesting feature of Fig.7 is that the minimum values of the damping derivative $n_{\dot{\psi}}$ are close to zero, for both the complete model and the body of revolution with fins removed. The minima occur at $x/\ell \approx 0.9$ for the complete model, and at $x/\ell \approx 0.6$ for the model without fins. There is at present no theoretical treatment which predicts this result. From the point of view of balloon stability, it is the values of the aerodynamic damping about the centre of gravity or the point of cable attachment, which are significant, and these will undoubtedly be positive.

Note that the only single derivative found from the dynamic tests is y_v, and one can compare this directly with the static value.

$$y_v \text{ (static)} = -1.43 \qquad y_v \text{ (dynamic)} = -1.04 .$$

The large lack of correspondence between these values is probably mainly due to the poor accuracy of inferring a value of y_v from the damping measurements about the three axes of the tests.

LIST OF SYMBOLS

ℓ length of balloon model

d maximum diameter of balloon model

$S = \frac{\pi d^2}{4}$ maximum cross sectional area of balloon model

α angle of incidence

β angle of sideslip

ρ density of free stream

LIST OF SYMBOLS (Contd.)

U velocity of free stream

x co-ordinate along model centre line

x_A distance of axis of rotation aft of reference origin

$C_L = \frac{L}{\frac{1}{2}\rho U^2 S}$ lift coefficient

$C_D = \frac{D}{\frac{1}{2}\rho U^2 S}$ drag coefficient

$C_m = \frac{M}{\frac{1}{2}\rho U^2 S\ell}$ pitching moment coefficient

$C_Y = \frac{Y}{\frac{1}{2}\rho U^2 S}$ side force coefficient

$C_n = \frac{N}{\frac{1}{2}\rho U^2 S\ell}$ yawing moment coefficient

lateral non-dimensional stability derivatives:-

$n_v = \frac{N_v}{\rho US\ell}$ $\qquad$ $y_v = \frac{Y_v}{\rho US}$

$n_r = \frac{N_r}{\rho US\ell^2}$ $\qquad$ $y_r = \frac{Y_r}{\rho US\ell}$

$n_{\dot{v}} = \frac{N_{\dot{v}}}{\rho S\ell 2}$ $\qquad$ $y_{\dot{v}} = \frac{Y_{\dot{v}}}{\rho S\ell}$

$n_{\dot{\psi}} = \frac{N_{\dot{\psi}}}{\rho US\ell^2}$

f frequency of oscillation (c.p.s.)

$\nu = \frac{2\pi f\ell}{U}$ non-dimensional frequency parameter.

LIST OF REFERENCES

No.	Author(s)	Title, etc.
1	Waters, M.H.L.	Some observations on the wander of a kite balloon. Unpublished M.O.A. Report.
2	Neumark, S.	Equilibrium configurations of flying cables of captive balloons, and cable derivatives for stability calculations. A.R.C. 23,244. June, 1961.
3	Neumark, S. Thorpe, A.W.	Theoretical requirements of tunnel experiments for determining stability derivatives in oscillatory longitudinal disturbances. A.R.C. R. & M. 2903. June, 1950.

APPENDIX

EXPRESSION FOR THE AERODYNAMIC YAWING MOMENT WHEN THE MODEL IS ROTATED ABOUT DIFFERENT AXES

Referring to Fig.3, the model is in rotation about a fixed axis A, a distance x_A aft of the origin O, to which the motion, forces, moments and stability derivatives are referred. The model is at an angular displacement ψ.

For ψ small, the motion of O is defined by:

$$v = x_A \dot{\psi} - U\psi \tag{7}$$

$$r = \dot{\psi} . \tag{8}$$

The aerodynamic moment about A is:

$$N_A = N + x_A Y \tag{9}$$

Now, with the assumptions of linear stability theory, we have:

$$\left.\begin{aligned} N &= N_v v + N_{\dot{v}} \dot{v} + N_r r + N_{\dot{r}} \dot{r} \\ Y &= Y_v v + Y_{\dot{v}} \dot{v} + Y_r r + Y_{\dot{r}} \dot{r} . \end{aligned}\right\} \tag{10}$$

Therefore

$$\begin{aligned} N_A &= (N_v + x_A Y_v) v + (N_{\dot{v}} + x_A Y_{\dot{v}}) \dot{v} + (N_r + x_A Y_r) r + (N_{\dot{r}} + x_A Y_{\dot{r}}) \dot{r} \\ &= (N_v + x_A Y_v) (x_A \dot{\psi} - U\psi) + (N_{\dot{v}} + x_A Y_{\dot{v}}) (x_A \ddot{\psi} - U\dot{\psi}) \\ &\quad + (N_r + x_A Y_r) \dot{\psi} + (N_{\dot{r}} + x_A Y_{\dot{r}}) \ddot{\psi} \\ &= - [U (N_v + x_A Y_v)] \psi + [x_A (N_v + x_A Y_v) - U(N_{\dot{v}} + x_A Y_{\dot{v}}) + (N_r + x_A Y_r)] \dot{\psi} \\ &\quad + [x_A (N_{\dot{v}} + x_A Y_{\dot{v}}) + (N_{\dot{r}} + x_A Y_{\dot{r}})] \ddot{\psi} , \end{aligned} \tag{11}$$

and the relationships (2, 3, 4) of section 2 follow.

The above derivation is similar to that given by Neumark and Thorpe[3] for longitudinal symmetric motion.

W.T.2078 C.P.643 K3. Printed in England.

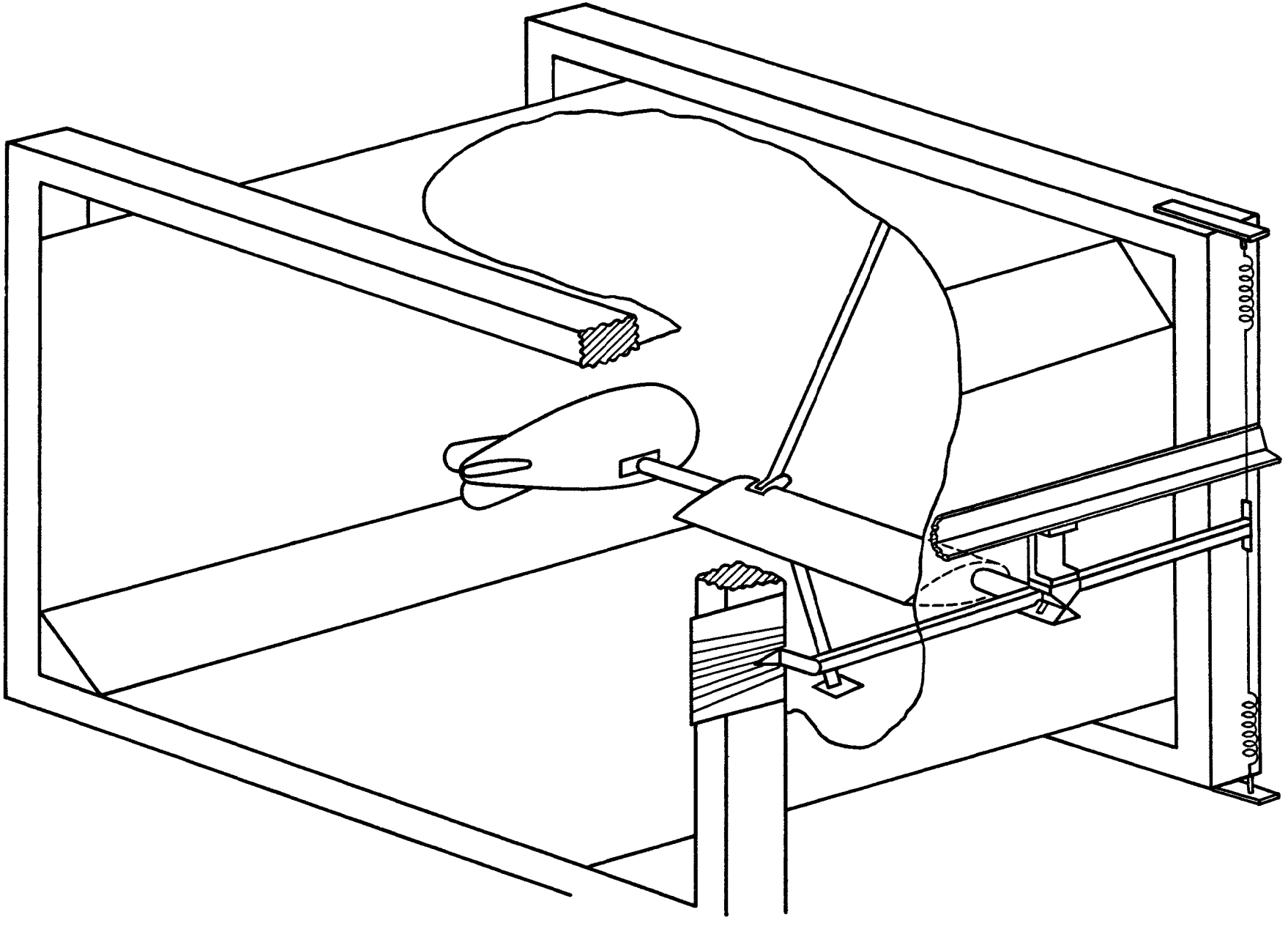

FIG. 1. THE DYNAMIC TEST RIG.

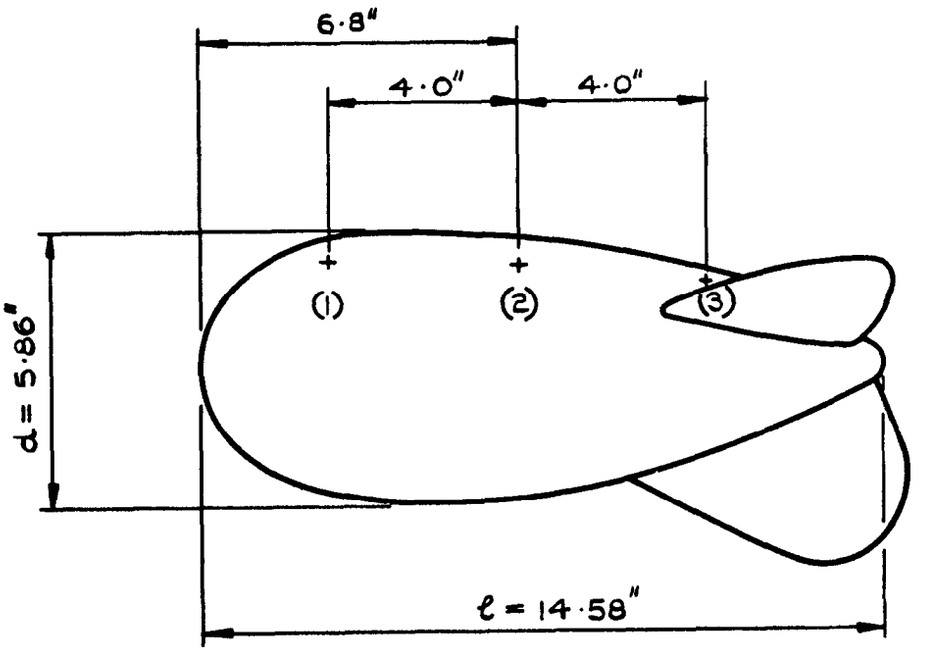

FIG 2. POSITIONS OF THE AXES OF ROTATION.

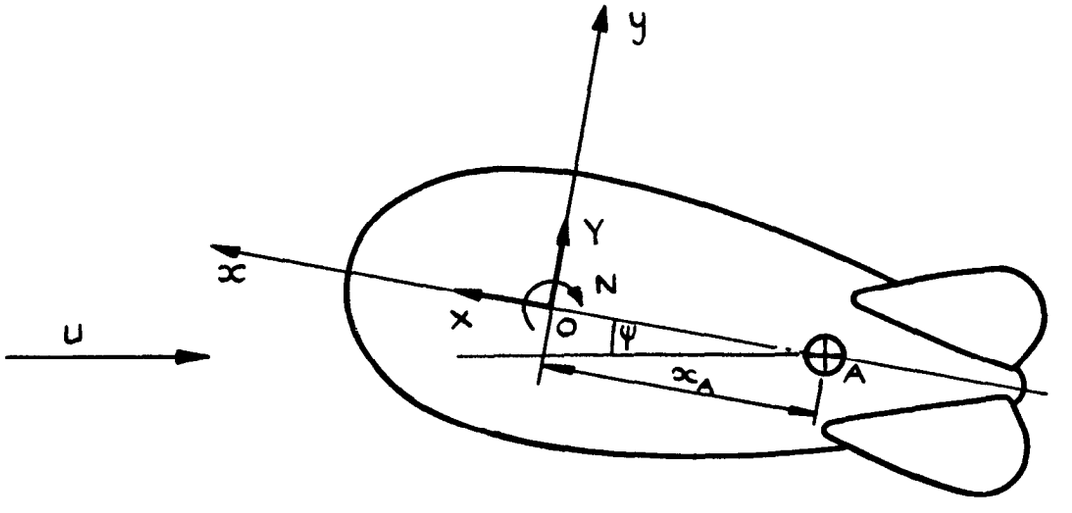

FIG. 3. REFERENCE AXES AND NOTATION.

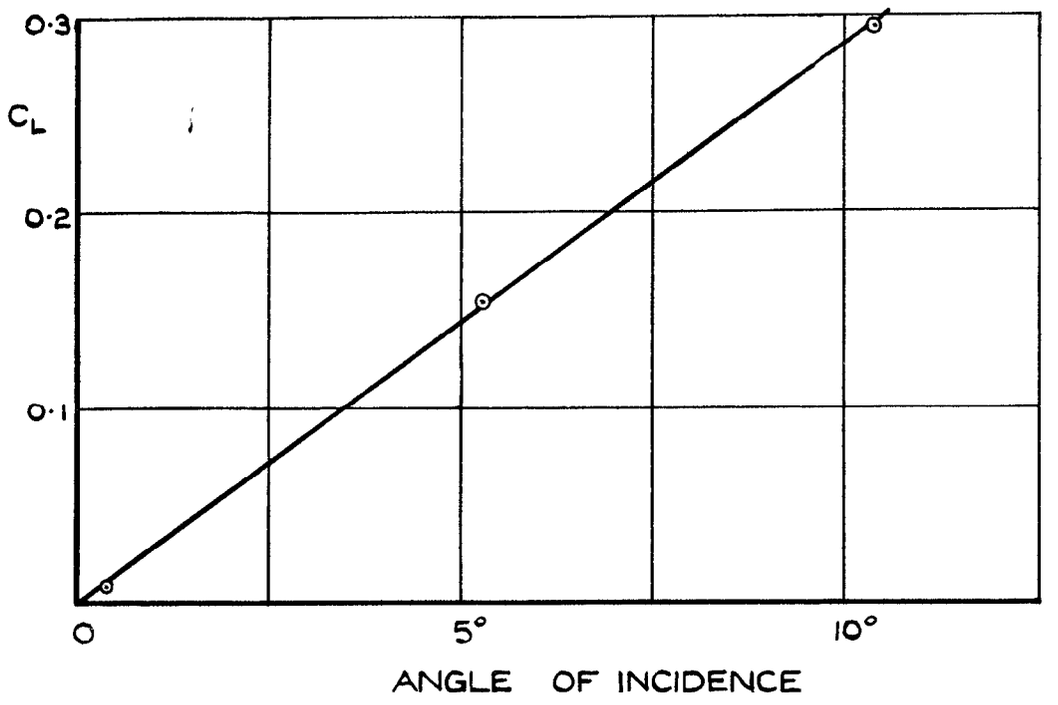

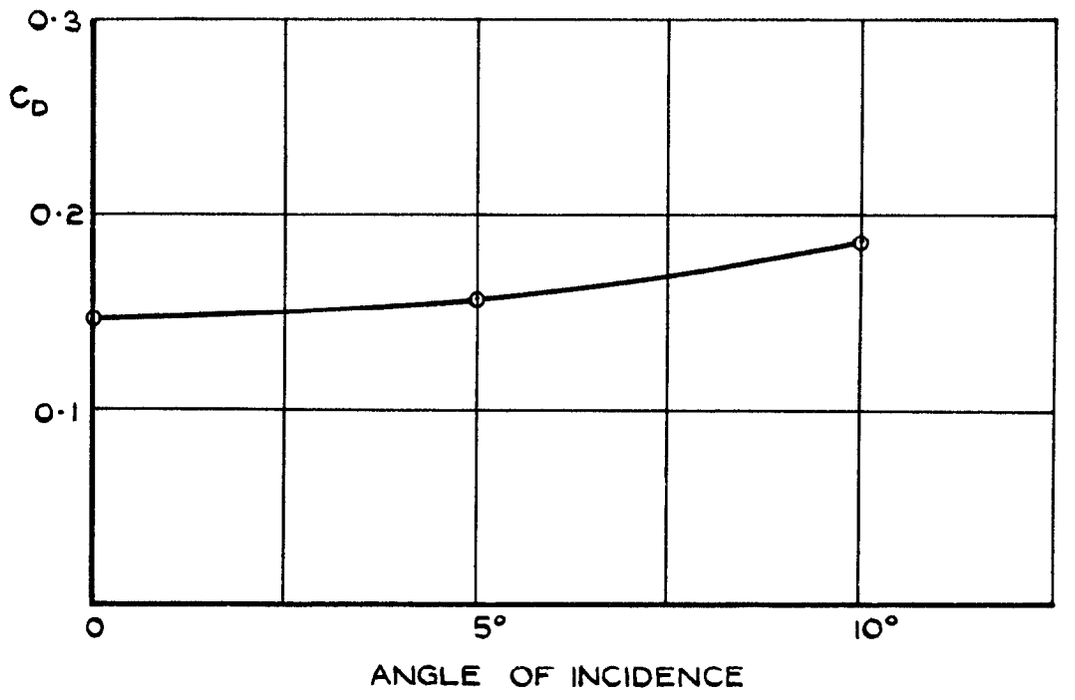

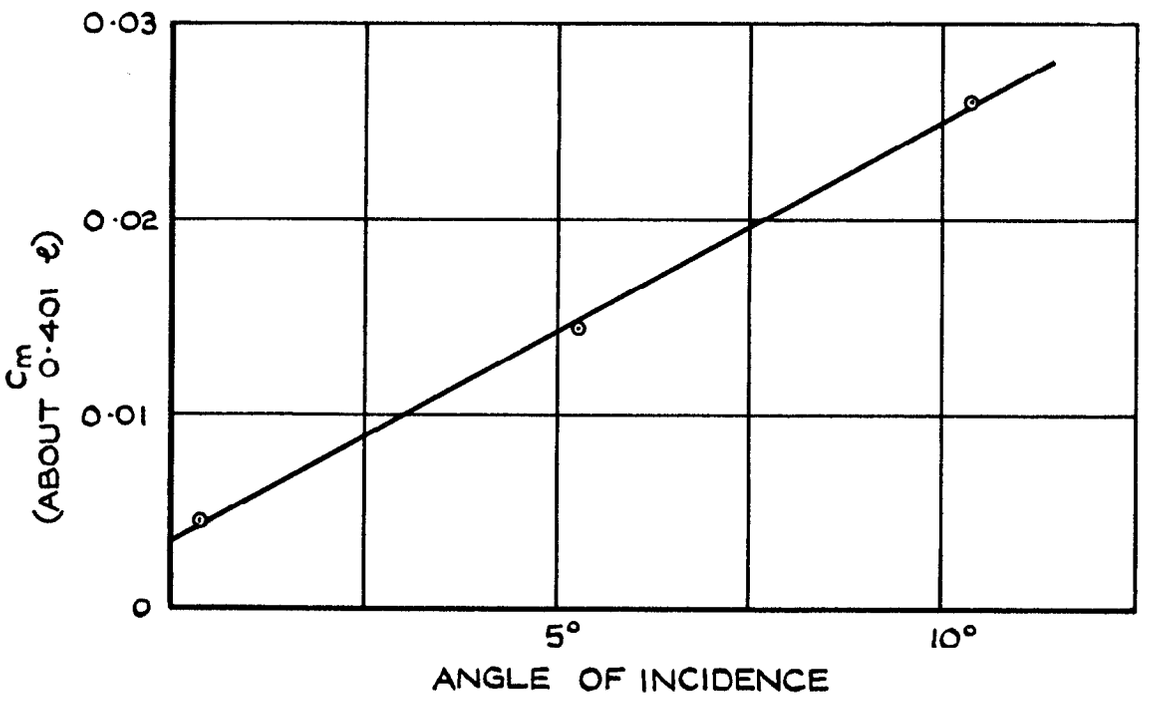

FIG. 4. LIFT, DRAG AND PITCHING MOMENT.

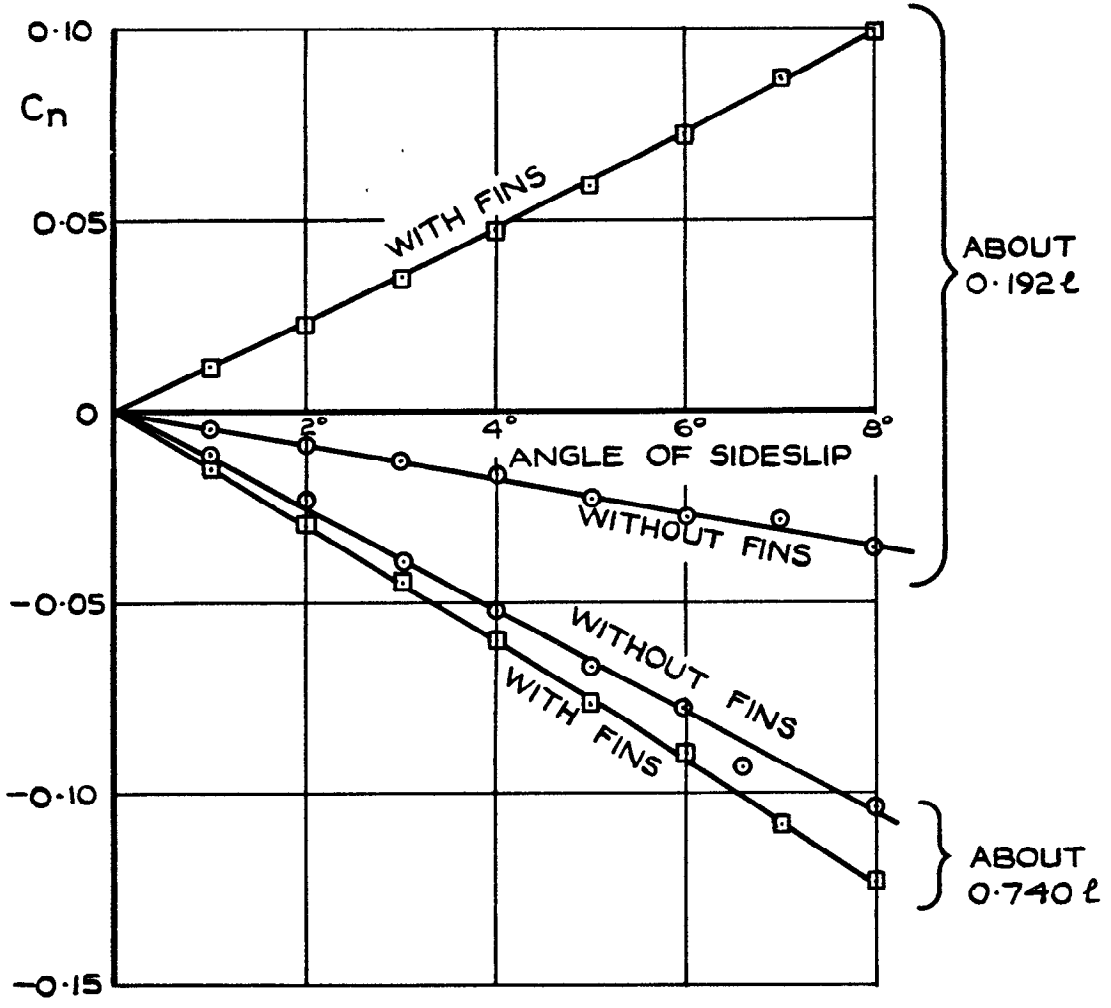

FIG. 5. VARIATION OF YAWING MOMENT WITH SIDESLIP; $\alpha = 0^\circ$

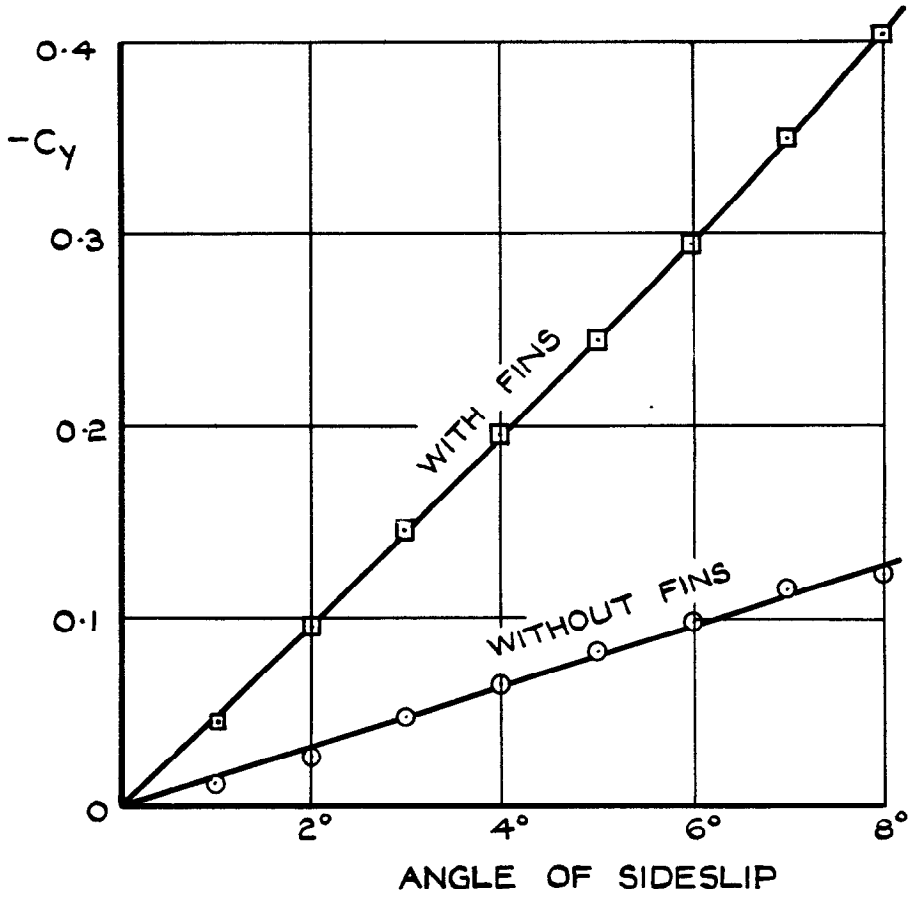

FIG. 6. VARIATION OF SIDE FORCE WITH SIDESLIP; $\alpha = 0^\circ$

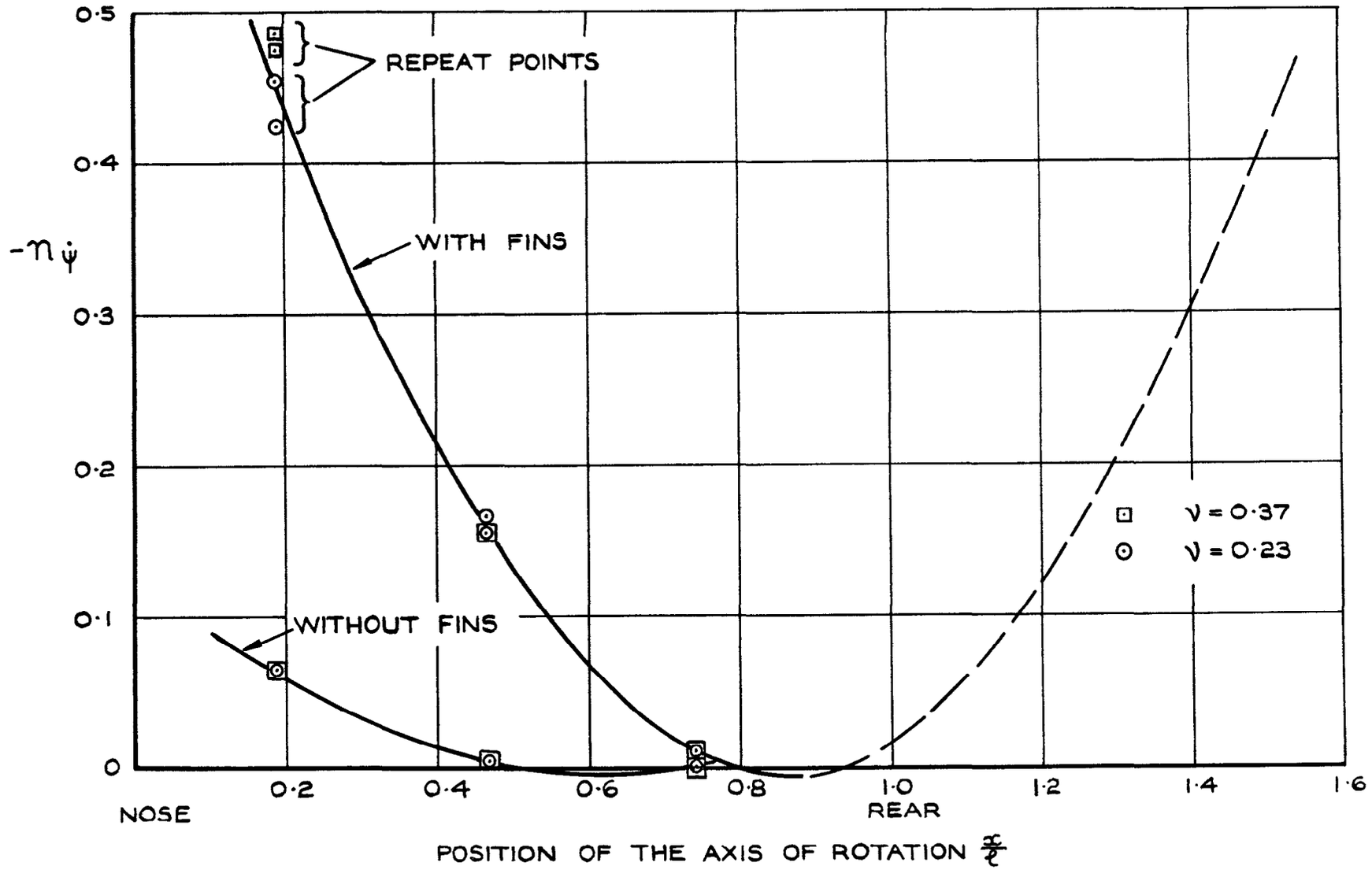

FIG. 7. AERODYNAMIC DAMPING IN YAW ABOUT VARIOUS AXES OF ROTATION; $\alpha = 0^{\circ}$

A.R.C. C.P. No. 643.

533.63:
533.6.013.1:
533.6.013.4

LOW SPEED WIND TUNNEL TESTS ON A KITE BALLOON MODEL.
Simonds, M.H. November 1961.

Low speed wind tunnel tests, aimed mainly at finding certain lateral aerodynamic stability derivatives, were carried out on a rigid 1/80th scale model of a 70600 cu ft kite balloon. The lift, drag and pitching moment, and the variation with angle of sideslip of the static values of side force and yawing moment, were found. In dynamic tests, the aerodynamic damping of free oscillations in yaw was measured about three separate axes of rotation. From these measurements the following combinations of stability derivatives were found: $(n_r - n_{\dot{v}})$, $(n_v - y_{\dot{v}} + y_r)$ and y_v. Results were obtained for the model at zero incidence, with the fins in place and with them removed.

A.R.C. C.P. No. 643

533.63:
533.6.013.1:
533.6.013.4

LOW SPEED WIND TUNNEL TESTS ON A KITE BALLOON MODEL.
Simonds, M.H. November 1961.

Low speed wind tunnel tests, aimed mainly at finding certain lateral aerodynamic stability derivatives, were carried out on a rigid 1/80th scale model of a 70600 cu ft kite balloon. The lift, drag and pitching moment, and the variation with angle of sideslip of the static values of side force and yawing moment, were found. In dynamic tests, the aerodynamic damping of free oscillations in yaw was measured about three separate axes of rotation. From these measurements the following combinations of stability derivatives were found: $(n_r - n_{\dot{v}})$, $(n_v - y_{\dot{v}} + y_r)$ and y_v. Results were obtained for the model at zero incidence, with the fins in place and with them removed.

A.R.C. C.P. No. 643

533.63:
533.6.013.1:
533.6.013.4

LOW SPEED WIND TUNNEL TESTS ON A KITE BALLOON MODEL.
Simonds, M.H. November 1961.

Low speed wind tunnel tests, aimed mainly at finding certain lateral aerodynamic stability derivatives, were carried out on a rigid 1/80th scale model of a 70600 cu ft kite balloon. The lift, drag and pitching moment, and the variation with angle of sideslip of the static values of side force and yawing moment, were found. In dynamic tests, the aerodynamic damping of free oscillations in yaw was measured about three separate axes of rotation. From these measurements the following combinations of stability derivatives were found: $(n_r - n_{\dot{v}})$, $(n_v - y_{\dot{v}} + y_r)$ and y_v. Results were obtained for the model at zero incidence, with the fins in place and with them removed.

© *Crown Copyright 1963*

Published by
HER MAJESTY'S STATIONERY OFFICE

To be purchased from
York House, Kingsway, London W.C.2
423 Oxford Street, London W.1
13A Castle Street, Edinburgh 2
109 St. Mary Street, Cardiff
39 King Street, Manchester 2
50 Fairfax Street, Bristol 1
35 Smallbrook, Ringway, Birmingham 5
80 Chichester Street, Belfast 1
or through any bookseller

Printed in England

S.O. CODE No. 23-9013-43